Strong isotopic labeling effects on the pressure dependent thermodynamics of polydimethylsiloxane/polyethylmethylsiloxane blends

Mario Beiner
FORTH-Institute of Electronic Structure and Laser, P.O. Box 1527, 71110 Heraklion, Crete, Greece and Universität Halle-Wittenberg, Fachbereich Physik, D-06099 Halle, Germany

George Fytas
FORTH-Institute of Electronic Structure and Laser, P.O. Box 1527, 71110 Heraklion, Crete, Greece and Max-Planck-Institut für Polymerforschung, P.O. Box 3148, D-55021 Mainz, Germany

Gerhard Meier
Max-Planck-Institut für Polymerforschung, P.O. Box 3148, D-55021 Mainz, Germany and Forschungszentrum Jülich, Institut für Festkörperforschung, P.O. Box 1913, D-52425 Jülich, Germany

Sanat Kumar
Department of Materials Science and Engineering, Pennsylvania State University, University Park, Pennsylvania 16802

(Received 9 August 2001; accepted 24 October 2001)

Using photon correlation spectroscopy we show that isotopic labeling can strongly alter the pressure dependent thermodynamics of polydimethylsiloxane/polyethylmethylsiloxane blends, while each blend enhances its miscibility upon pressurization up to 2 kbar. The pressure dependence of the Flory interaction parameter, χ, changes by a factor of 4 when the deuteration of side groups is switched from one polymer to the other, but its pressure dependence is always negative. These results may be understood as being driven by the very different negative excess volumes of mixing for these different isotopic blends. We have attempted to unify our understanding of the role of pressure on blend thermodynamics into a single master plot by examining our data on volume changes on mixing vs the interaction parameter for the polysiloxane blends, and those from neutron scattering experiments on polyolefin blends and on a blend of a polyolefin and a polysiloxane. We find no universal trends when examined on this basis, and instead observe that variations in the chemical identity of the polymers in question and their chain lengths lead to very different plots. Further, since both neutron scattering and light scattering provide the same qualitative results, we argue that these results are not artefacts of either experimental technique. Our results strongly argue that the role of pressure on blend thermodynamics are much more complex than previously anticipated, and stress the need for improved theories for this important class of experiments. [DOI: 10.1063/1.1428346]

I. INTRODUCTION

Previously,[1,2] it has been shown that pressure can enhance the miscibility of model blends which exhibit upper critical solution temperature (UCST) behavior.[3] These results are surprising since most typical UCST blends demonstrate the opposite behavior, i.e., $\partial T_c/\partial P \geqslant 0$.[4,5] The observed compatibilization upon compression for the polyethylmethylsiloxane (PEMS)/polydimethylsiloxane (PDMS) blend, i.e., $\partial T_c/\partial P \approx -25$ K/kbar,[1] has been unambiguously attributed to its negative volume change on mixing, ΔV, which was measured on identical samples.[6] In contrast, most UCST blends possess $\Delta V \geqslant 0$,[7] providing a basis for explaining the decreased miscibility of typical polymer blends on pressurization.

The role of pressure on the thermodynamics of polymer blends can be understood by a straightforward extension of the Flory–Huggins free energy of mixing two polymers per lattice site, ΔG_{mix},[8,9]

$$\frac{\Delta G_{\mathrm{mix}}}{v_0 RT} = \frac{\phi}{N_A v_A}\ln\phi + \frac{(1-\phi)}{N_B v_B}\ln(1-\phi) + \frac{\chi}{v_0}\phi(1-\phi). \tag{1}$$

Here N_i and v_i are the degree of polymerization and the molar volume for species i, respectively, ϕ is the volume fraction of species A, and v_0 is a reference volume. χ is the interaction parameter which includes all of the consequences of pressurization on blend thermodynamics. Lefebvre *et al.*[7] and Kumar[9] showed that, to better than 1%, the role of pressure is captured by the simple relationship,

$$\chi(P) = \chi(P=0) - \frac{P v_0}{2RT}\left[\frac{\partial^2(\Delta V/v_{\mathrm{incom}})}{\partial\phi^2}\right]_{T,P}, \tag{2}$$

where v_{incom} is the molar volume of a hypothetical mixture which has no volume change on mixing. This equation can be derived by using the Maxwell relationship $\partial^3\Delta G_{\mathrm{mix}}/\partial\phi^2\partial P = \partial^3\Delta G_{\mathrm{mix}}/\partial P\partial\phi^2$ and postulating that the resulting derivative on the right-hand side is pressure inde-

TABLE I. Sample characteristics.

Code	N_{PDMS}	N_{PEMS}	M_w^{PDMS} (g mol^{-1})	M_w^{PEMS} (g mol^{-1})	Φ_{PDMS}	T_c
d-M/h-E	224	259	17 850	22 000	0.52	≈122
h-M/h-E	263	275	19 450	24 250	0.51	62
h-M/d-E	210	262	20 000	21 500	0.53	≈40

pendent. Note that the application of this Maxwell equation using the experimentally derived values of χ is not affected by fluctuations, and hence the Ginsburg criterion, for any chosen blend. Thus Eq. (2) may be regarded as a generally applicable relationship for systems with low compressibility, i.e., far from their gas–liquid critical points. For PDMS/PEMS, characterized by $\Delta V = \underline{\nu} v_{\mathrm{incom}} \phi(1-\phi)$, it follows from Eq. (2) that

$$\left[\frac{\partial \chi}{\partial P}\right]_T = \frac{v_0}{RT}\underline{\nu}. \tag{3}$$

Since experiments for the PEMS/PDMS blend show that $\underline{\nu} = -3\times10^{-2}$ and $(\partial\chi/\partial P)_{T,\phi} = -5\times10^{-6}\,\mathrm{bar}^{-1}$, Eq. (3) is obeyed remarkably well by this model system. In addition to suggesting the experimental applicability of Eq. (3), Ref. 7 has also shown the additional result that $\underline{\nu}$ scales with the $\chi(P=0)$ for a class of saturated hydrocarbon polymers. The constant of proportionality between these quantities which describes experimental data is unknown, even though this proportionality was derived on general thermodynamic grounds 65 years ago.[10,11] More recently Kumar[9] showed for systems which obeyed regular solution theory,

$$\underline{\nu} \simeq \chi(P=0)\frac{\kappa_T RT}{v_0}, \tag{3a}$$

where κ_T is the isothermal compressibility of the liquid. If obeyed by real systems, this implies that a corresponding states principle, based on a single variable, can explain the role of pressure on the thermodynamics of the idealized polyolefin blend systems.[12] The application of Eq. (3a) to typical polyolefins can be made by assigning $\kappa_T = 0.06\,\mathrm{kbar}^{-1}$, $v_0 = 150\,\mathrm{cm}^3/\mathrm{mol}$ and $T = 400\,\mathrm{K}$. This suggests that $\underline{\nu} = 0.013\chi(P=0)$, which should be contrasted with the experimental results,[7] $\underline{\nu} = 0.17\chi(P=0) - 7.6\times10^{-5}$. Thus, the physics embodied in Eq. (3a) misses important features of the experimental data, and the role of pressure on system thermodynamics remains poorly enunciated at this time.

To better understand the role of pressure on blend thermodynamics, we have extended our light scattering work on *h*-PDMS [*h-M*]/*h*-PEMS [*h-E*],[1] to *h-M*/*d*-PEMS [*d-E*] and *d*-PDMS [*d-M*]/*h-E* blends each comprised of chain with very similar lengths. We have employed photon correlation spectroscopy to elucidate the pressure dependence of the Flory interaction parameter, χ, and from there estimate the excess volume change on mixing of this blend [using Eq. (3)]. We then show that $\underline{\nu}$ does correlate with $\chi(P=0)$, as expected, but that the slopes of the lines for the different isotopic blends considered *depend strongly on the chemical identities and chain lengths of the polymers in question*. These results illustrate that pressurization of polymer blends may not be understood in a simple corresponding states manner, and implies that pressure effects on blend thermodynamics are more complicated than anticipated based on past experiments.

II. EXPERIMENT

A. Sample preparation

The various polymers used were synthesized by anionic polymerization (see, e.g., Ref. 13). Accordingly, relatively sharp fractions of material are obtained which are analyzed by gel permeation chromatography for the molecular weight distribution. The parameters resulting from this analysis are summarized in Table I. We prepared samples with their critical composition, as derived from the mean-field prediction, i.e., $\phi_c = N_{\mathrm{PEMS}}^{1/2}/(N_{\mathrm{PDMS}}^{1/2} + N_{\mathrm{PEMS}}^{1/2})$ for PDMS. Proper amounts of polymers were dissolved in *n*-hexane and filtered through Millipore Teflon filters (0.22 μm) into a $\frac{1}{2}$ in. o.d. dust free light scattering cell. To remove the solvent the samples were held under vacuum for several days at $T > T_c$. Note that, as expected from past work, switches in isotopic labeling dramatically alter the critical temperatures of these blends.

B. Experimental setup

Hydrostatic pressure in the range 1–1750 bar is applied by compressing nitrogen gas from a Nova Swiss membrane compressor. To ensure that no gas will diffuse through the sample to the position of measurement (at the bottom of the cell), a diffusion path of 2 cm length is attached on top of the sample in the form of a moving piston. The piston is sealed by a Viton O-ring to the inner surface of the cell. Since the diffusion coefficient of N_2 in liquids is of the order of $10^{-5}\,\mathrm{cm}^2/\mathrm{s}$ at ambient P, we estimate the time for a safe experiment to be ~6 h.

The light scattering cell used for this study is identical to the one which has been described previously.[14] We have used an argon ion laser (Spectra Physics) operating at $\lambda = 488\,\mathrm{nm}$. The incident polarization is vertical V. Mono mode fibres were placed close to the optical windows of the pressure cell, and their output fed into the input of an ALV monitoring system essential for measuring the full autocorrelation function of the scattered light intensity with an ALV 5000 correlator. While no analyzer was used, nevertheless, the polarization of the scattered light is V to a very good approximation since PDMS and PEMS exhibit almost no depolarized scattering (about two orders of magnitude smaller than R_{VV} of toluene). All intensities were measured with respect to toluene thereby using the Rayleigh ratio of $R_{VV}^{\mathrm{Tol}} = 3.96\times10^{-6}\,\mathrm{cm}^{-1}$.

C. Data treatment

The static structure factor $S(q)$ is obtained from $I(q)$ via

$$S(q) = \frac{I(q)\lambda^4 \rho N_L R_{VV}^{\mathrm{Tol}}}{I_{\mathrm{Tol}} n_{\mathrm{Tol}}^2 4\pi^2 (n_A - n_B)^2 M_{\mathrm{mon}}}, \tag{4}$$

where N_L is the Avogadro number, $\rho=\phi_A\rho_A+\phi_B\rho_B$, the density ($A$,$B$: components) n the index of refraction of the appropriate species, and $M_{\mathrm{mon}}=\phi_A M_A^{\mathrm{mon}}+\phi_B M_B^{\mathrm{mon}}$ the monomer molar mass. I_{tol} and n_{Tol} are the intensity and refractive index of the toluene standard. The desired autocorrelation function of the scattered electric field $g(q,t)$ is related to the measured intensity time correlation function $G(q,t)$ through the Siegert relation,

$$G(q,t)=\langle I(q)\rangle^2\{1+f\alpha^2|g(q,t)|^2\}, \tag{5}$$

where $\langle I(q)\rangle$ is the mean intensity, f is an instrumental factor, and α is the fraction of the totally scattered intensity, $I_c(q)/I(q)$, arising from concentration fluctuations $\phi_q(t)$. $g(q,t)=\langle\phi_q(t)\phi_{-q}(0)\rangle=S(q,t)/S(q)$ is identified as the concentration autocorrelation function where $S(q,t)$ is the dynamic and $S(q)=\langle|\phi_q(0)|^2\rangle$ is the static structure factor. The time evolution of $S(q,t)$ is given by

$$S(q,t)=S(q)\exp(-\Gamma(q)t), \tag{6}$$

with $\Gamma(q)$ being the Rayleigh linewidth, which is identified with the collective thermal decay rate of composition fluctuations $\phi_q(t)$. Figure 1 shows the experimental $S(q,t)/S(q)$ for the polymer blends *d-M/h-E* at 105 °C, *h-M/h-E* (sample A in Ref. 1) at 50 °C and *h-M/d-E* at 40 °C, respectively, at different pressures P. All relaxation functions decay exponentially, in agreement with Eq. (6), yielding the diffusive (q^2-dependent) rate $\Gamma(q)$.

At low wave vectors $q\to 0, S(q\to 0)\equiv S(0)=(\partial^2\Delta G/kT/\partial\phi^2)_{T,P}$ and Eq. (1) leads to

$$S(0)^{-1}=2(\chi_s-\chi(T,P)) \tag{7}$$

with $2\chi_s=(\phi_A N_A)^{-1}+(\phi_B N_B)^{-1}$, the value of the interaction parameter at the spinodal. Furthermore $\Gamma(q)$ is connected to thermodynamics via the random phase approximation,

$$\Gamma(q)=\phi(1-\phi)\frac{\Lambda}{S(0)}q^2, \tag{8}$$

where Λ is the purely kinetic Onsager coefficient, which is proportional to the local segmental mobility w_0.[15] Access to both the interdiffusion coefficient $D=\Gamma(q)/q^2$ and $S(0)\propto I_c$ in the limit $q\to 0$ is possible through our dynamic light scattering experiment and provides complementary, self-consistent information which is not possible to get by other methods like SANS.

III. RESULTS

As noted above, the intermediate scattering function $S(q,t)$ is well described by Eq. (6) yielding the interdiffusion coefficient $D=\Gamma(q)/q^2$. In all three cases, we clearly observe an unexpected speeding up of $S(q,t)$ with increasing P shown up to $P=400$ bar (Fig. 1). Above this pressure, the kinetic effect, i.e., the reduced mobility cancels the thermodynamic effect of P. The latter is reflected in the static structure factor $S(0)$, which sharply increases with decreasing P below 400 bar (Fig. 1). Figure 2 clearly demonstrates that pressure compatibilizes this polysiloxane blends. As previously shown in Ref. 1, the decrease of $S(0)$ with P is responsible for the increase of Γ [Eq. (8)] and hence the speeding up of $S(q,t)$ in Fig. 1. Obviously the pressure effect on thermodynamics overcomes the countereffect of P on the mobility [Λ in Eq. (8)], at least in the vicinity of $T_c(P)$. At higher P the influence on the mobility term may become important as found in a low molecular mass *h-M/h-E* blend (system C in Ref. 1), where dynamic data was collected for $T>T_c+100$ K.

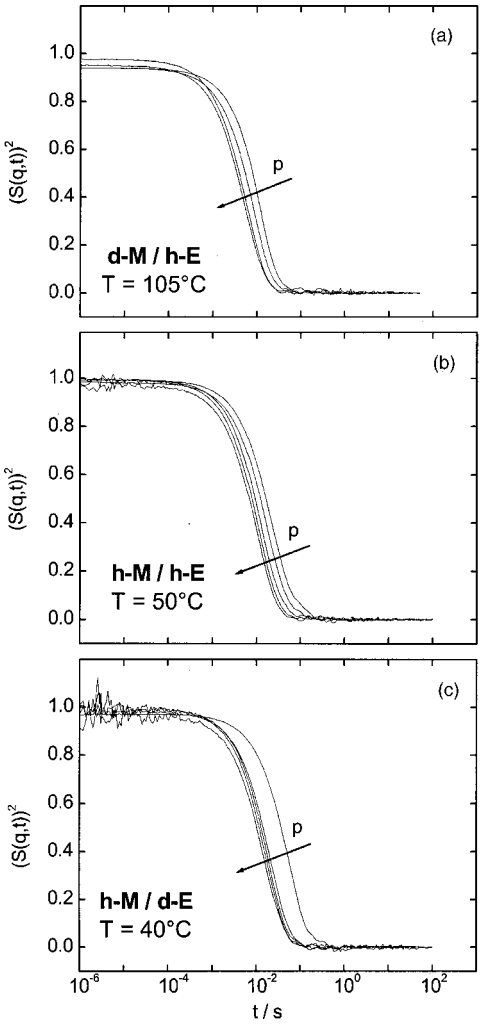

FIG. 1. The dynamic structure factor $S(q,t)$ as a function of logt for sample *d-M/h-E* at $T=105$ °C (a), *h-M/h-E* at $T=50$ °C (b), and *h-M/d-E* at $T=40$ °C (c). T for $q=0.034$ nm^{-1} and various pressures in increasing order as indicated by the arrow: P/bar: 175, 200, 240, 400 (a); P/bar: 125, 150, 200, 300, 400 (b); P/bar: 1, 100, 200, 300, 400 (c). The lines connect the experimental points.

While our data in Fig. 2 show that pressure effects lead to a stabilization of blend miscibility at low pressure, data at high pressures (up to 1750 bar) for the most immiscible blend, *d-M/h-E* (for code, see Table I), appear to suggest a flattening or even a slight increase of $S(0)$ with P. This trend of increasing $S(0)$ with P is a sign of incompatibilization, which was a typical case in polymer blends,[4] and tentatively suggests that re-entrant pressure dependent behavior might be feasible at even higher pressures. It should also be noted that this behavior is different in block copolymer systems,[16] where a re-entry in the phase diagram with a clear intensity minimum was found. However, block copolymer systems are

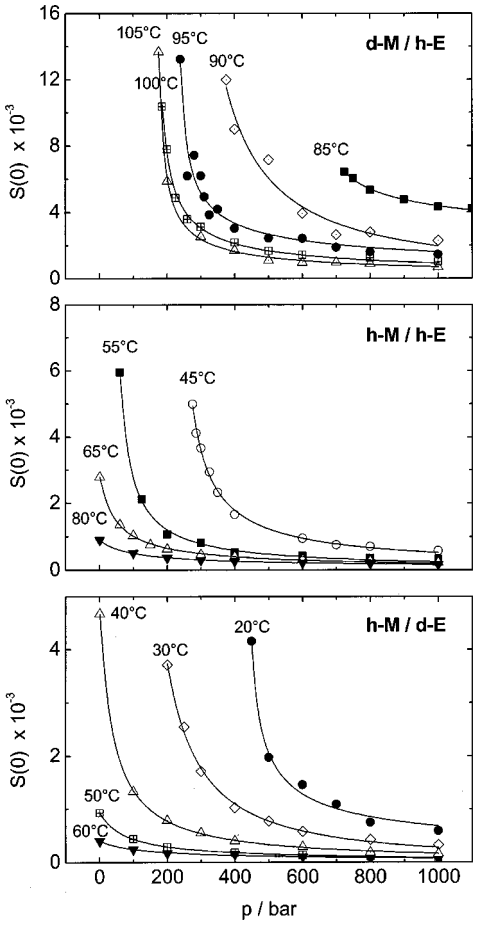

FIG. 2. The static structure factor $S(0)$ as a function of pressure for various temperatures as indicated in the plot. The lines are to guide the eye.

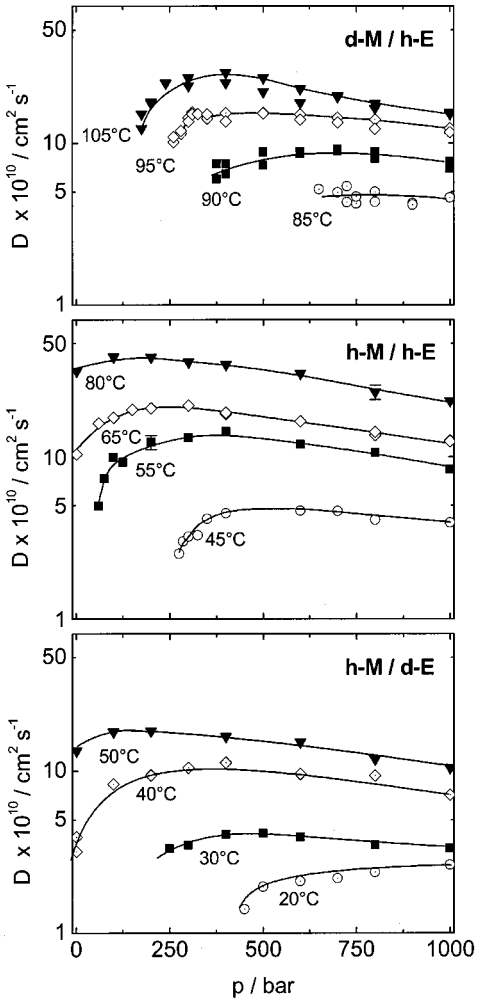

FIG. 3. The interdiffusion coefficient D as a function of pressure for various temperatures as indicated in the plot. The lines are to guide the eye.

truly one component systems and can not be compared with blends, which are regular physical mixtures.

The effect of pressure on the material dependent properties is demonstrated in Fig. 3, where D is plotted against P for various T's for all three blends considered. The maximum of the function $D(P)$ was found to shift to elevated P with decreasing T clearly indicating that higher P is needed to mix at low T. The shift of the phase boundary to lower T with P is evident as high $S(0)$ values (cf. Fig. 2) are attained only at lower T with increasing P.

Whether thermodynamics alone fully accounts for the critical behavior of interdiffusion can be checked from the monotonic dependence of purely kinetic coefficient Λ with T and P according to Eq. (8). For the blend h-M/h-E,[1] $\Lambda(T,P)$ displays no extremum, and exhibits a rather weak T- and P-dependence, which is the expected behavior for a blend that is far from T_g and T_c.[15] The activation volume $\Delta V^{\#}=RT(\partial \ln \Lambda/\partial P)_T$ and the activation energy $\Delta E=R(\partial \ln \Lambda/\partial(1/T))_P$ quantify the P and T dependence of Λ in the pressure range 500–1000 bar. $\Delta V^{\#}$ for the three blends assumes a very similar value of 60 ± 4 cm^3/mol. In contrast, the low activation energy, ΔE, is associated with larger errors and does not yield meaningful trends. A reliable estimate of ΔE at constant P can be obtained from the values of Λ in d-M/h-E (at high T), h-M/h-E (intermediate T), and d-M/d-E (at low T). Thus an Arrhenius temperature dependence of Λ at 90 °C, 65 °C, and 40 °C from the data in Figs. 2 and 4 leads to $\Delta E=16\pm5$ kJ/mol. The speed up effect of pressure on $S(q,t)$ in Fig. 1 is therefore of purely thermodynamic origin.

In Fig. 4 we plot $1/S(T,P)$ vs $1/T$ [Eq. (7)] at various pressures to obtain the enthalpic, χ_h, and entropic, χ_σ, contributions to the Flory parameter, χ,

$$\chi=\frac{\chi_h}{T}-\chi_\sigma. \tag{9}$$

For the three blends, $1/S(T,P)$ decreases linearly with $1/T$ supporting the validity of Eq. (9) in this context. In agreement with past work,[1,4,7] and with theoretical expectations,[9,17] Fig. 5 shows that $S^{-1}(P,T)$, and hence χ, vary linearly with pressure. In contrast to experimental results on typical UCST polymer blends,[4] χ decreases with P in accordance with the observed compatibilization effect of P. We find $(\partial\chi/\partial P)_{T,P}=-4.7\times10^{-6}$ atm^{-1} at 50 °C for h-M/d-E, -2.3×10^{-6} atm^{-1} for h-M/h-E at 80 °C, and -1.0×10^{-6} atm^{-1} for d-M/h-E at 105 °C. These results are in the same range as the $(\partial\chi/\partial P)_{T,P}=-14\times10^{-6}$ obtained from SANS for the PEE/PDMS blend[2] at atmospheric pressure and $T=144$ °C. The overall $(\partial\chi/\partial P)<0$ results from

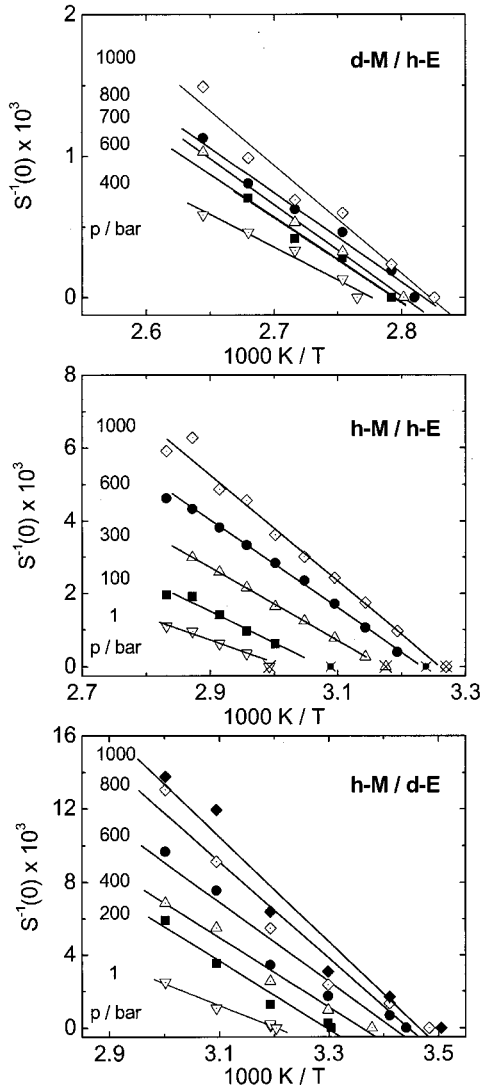

FIG. 4. The inverse structure factor $S^{-1}(0)$ vs $1/T$ at different pressures as indicated in the plot. The solid line represents linear fits of the mean field Eq. (7) to the data. The temperatures at $S^{-1}(0)=0$ are experimental values obtained from turbidity measurements. Sample code as in Fig. 1.

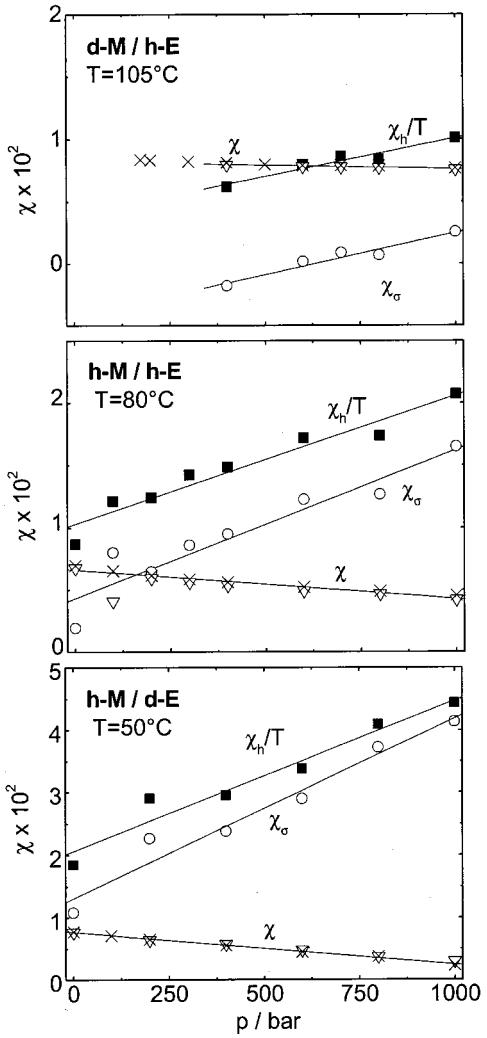

FIG. 5. Variation of the computed interaction parameter χ from the enthalpic part χ_h/T and entropic part χ_σ (obtained from the intercepts and slopes of Fig. 4 at different pressures) at $T=105$ °C (top), $T=80$ °C (middle), and $T=50$ °C (bottom) at different pressures where the symbols ∇ denote the computed values of $\chi=\chi_h/T-\chi_\sigma$). Sample code as in Fig. 1.

an increase of both χ_h and χ_σ with P, whereas for the cases where $(\partial\chi/\partial P)>0$, it was found that $\partial\chi_h/\partial P\simeq 0$ and $\partial\chi_\sigma/\partial P<0$.

For *h-M/h-E*, we have previously illustrated that $(\partial\chi/\partial P)_{T,\phi}$ is in agreement with the negative volume change of mixing as described in Eq. (3a). From Eq. (3a) we obtain $\underline{\nu}v_{\text{incom}}=-12.4\times10^{-2}$ cm^3/mol for *h-M/d-E*, -6.5×10^{-2} cm^3/mol for *h-M/h-E*, and -3.6×10^{-2} cm^3/mol for *d-M/h-E*. While $\chi(T)$ at 1 bar increases only by 20%, $|\underline{\nu}|$ becomes more than three times larger from *d-M/h-E* to *h-M/d-E* at the corresponding temperature of Fig. 5. Use of Eqs. (3) and (3a) suggests that $(\partial\chi/\partial P)_{T,\phi}=\chi[P=0]\kappa_T$. Since the isothermal compressibility of a polymer liquid does not change significantly for such changes in temperature, our results show that the regular solution approach cannot describe the behavior of these systems on pressurization. This point has been appreciated before.[7]

Figure 6 shows the temperature T_c at which the onset of visible phase separation in our blends was observed for a range of pressures. Since the systems respond very fast to pressure changes we chose to determine the pressure P_c below which a phase separation occurs at a given T_c. These turbidity temperatures are similar within experimental uncer-

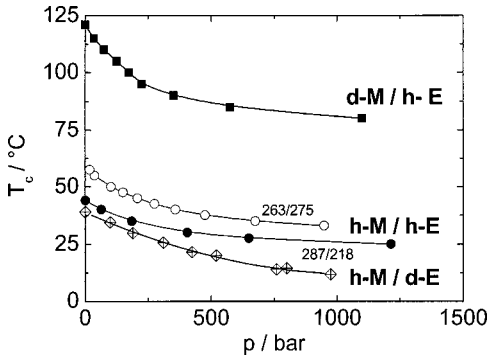

FIG. 6. Demixing curves for the blends under study. The two phase region is below the respective solid line. For the system *h-M/h-E* two pairs of *N* are given being code *A*, *B* from Beiner *et al.* (Ref. 1).

TABLE II. The interaction parameter, $\chi(T,P)=\chi(T)_{p=1\ \mathrm{bar}}+(\partial\chi/\partial p)P$.

Blend	*d-M/h-E*	*h-M/h-E*	*h-M/d-E*
$\chi(T)_{p=1\ \mathrm{bar}}\cdot 10^3=$	$\frac{(0.19\pm0.17)10^3}{T}+(7.82\pm0.44)$	$\frac{(3.15\pm0.11)10^3}{T}-(1.94\pm0.34)$	$\frac{(6.85\pm0.44)10^3}{T}-(13.4\pm1.5)$
$\left(\frac{\partial\chi}{\partial p}\right)\cdot 10^6\ \mathrm{bar}^{-1}=$	$\frac{(4.7\pm0.3)10^3}{T}-(13.5\pm0.7)$	$\frac{(4.4\pm0.3)10^3}{T}-(13.5\pm0.7)$	$\frac{(1.4\pm0.1)10^4}{T}-(47\pm3)$

tainties with those from the extrapolated $S^{-1}(0)\rightarrow 0$ in Fig. 4. All samples display $\partial T_c/\partial P\langle 0$ despite the fact that the mixing is exothermic. The observed pressure effect is significant, ~25 K/kbar (even larger for *d-M/h-E*), which is comparable in magnitude to those reported for other UCST systems where pressure induces demixing.

IV. DISCUSSION

To obtain a unified understanding of the role of pressure on blend dynamics, we compare and contrast our data to those on polyolefin blends presented recently by Lefebvre *et al.*[7] and on a polyolefin/polysiloxane blend presented by Schwahn *et al.*[2] In particular, we shall examine if a relationship similar to Eq. (3a), i.e., $\chi(P=0)\propto \underline{\nu}$, can describe all sets of data.

The $\chi(T,P)$ for the three blends considered here, as obtained from the static structure factor of Fig. 4 can be computed from $\chi(T,P=0)$ and $\partial\chi/\partial p$. The temperature dependences of these two quantities for each blend are listed in Table II. The χ for the PEMS/PDMS blend displays a stronger pressure dependence at lower temperatures [Fig. 7(a)]. Further, *h-M/d-E* exhibits the strongest and *d-M/h-E* the weakest *P*-dependence of χ among the three blends. Figure 7(a) further shows that $(\partial\chi/\partial P)$ is different for all three blends, contrary to the $(\partial\chi/\partial P)$ in four polymethylbutylene/polyethylbutylene blends only depended on $\chi(P=0)$ and is independent of ϕ and *N*. In these polyolefin blends, pressure induces incompatibilization and hence $\nu>0$.[7] However, in both systems $(\partial\chi/\partial P)_{T,\phi}$ increases with $1/T$.

In Fig. 7(b) the χ values at $P=1$ bar are plotted vs $1/T$ for the three polysiloxane blends. Clearly, these values are rather different, reflecting the disparity depicted in Fig. 7(a). The first concern when one views these data is if the light scattering experiments, or the differences in analysis procedure between light scattering and SANS, may yield these unusual results. SANS was used to determine χ values at 1 bar for the *h-M/d-E* and *d-M/h-E* blends.[18] The SANS derived χ values $\chi=4.7/T$-0.004 for *d-M/h-E* ($T\sim 140-230\,^{\circ}\mathrm{C}$) and $\chi=7.8/T$-0.018 for *h-M/d-E* ($T\sim 70-140\,^{\circ}\mathrm{C}$), compare favorably with the data in Fig. 7(b) extrapolated to these ranges. To further confirm that the analysis procedure in light scattering does not distort our findings, we have reanalyzed our light scattering data using the standard procedure employed in SANS. Since we find effectively no change, within experimental uncertainty, in the derived χ values at least at 1 bar pressure it is clear that the light scattering derived χ values are unambiguous.

Two questions now remain to be addressed in light of the experimental results discussed in this paper. First, we need to understand the strong isotope effect on the χ parameter, and also on its pressure dependence. Second, we need to understand the general applicability of the results reported here. That is, we need to know if $\underline{\nu}$ values scale linearly with $\chi(P=0)$, as suggested by Lefebvre *et al.*,[7] and if the dependence is system independent.

To probe the first question we refer to recent work by

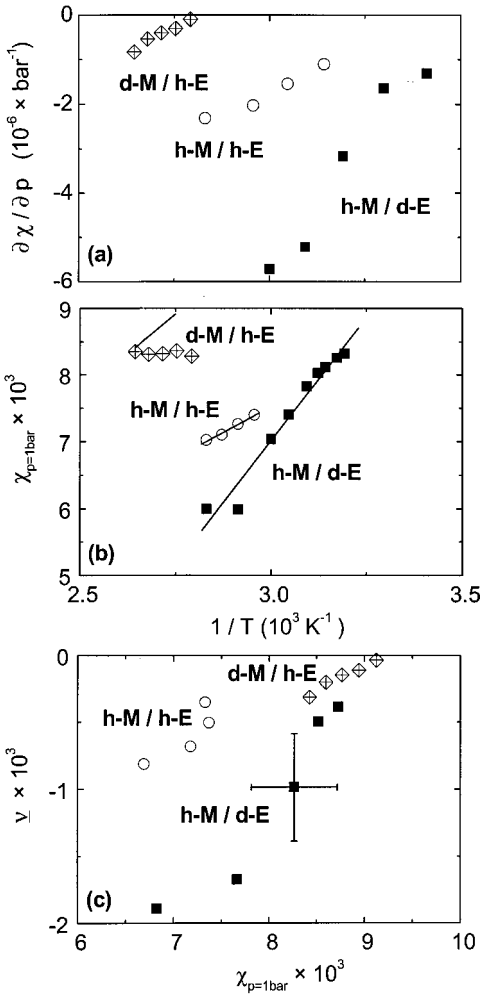

FIG. 7. (a) The pressure derivative of the interaction parameter χ vs the inverse temperature. (b) The χ-parameter at ambient pressure as a function of the inverse temperature and (c) relationship between the parameter $\underline{\nu}/\underline{\nu}_0$ for the volume change of mixing and the $\chi(P=0)$ for the three samples as indicated in the plot. The solid line in (b) indicates extrapolated χ values obtained for *d-M/h-E* from SANS (Ref. 18).

Krishnamoorti and co-workers[19] who had suggested that swapping isotope labeling between the two components of a blend lead to changes in miscibility that were explainable through changes in the solubility parameter on deuteration. To elaborate with particular emphasis on our example, we note that $h\text{-}M/d\text{-}E$ is the most soluble blend, while $d\text{-}M/h\text{-}E$ is the least soluble. Krishnamoorti *et al.*[19] suggest that deuterating a polymer would lower its solubility parameter, δ. Based on this statement and the regular solution definition of $\chi \sim (\delta_1 - \delta_2)^2$, it would be reasonable to conclude that $\delta_{hM} < \delta_{hE}$, and further than $\delta_{dM} < \delta_{hM}$, and $\delta_{dE} < \delta_{hE}$. There is one complicating factor, however, which prevents us from using this approach further to understand the experimental results presented here. Previous work by Beaucage *et al.*[20] has shown that the isotopic χ parameter in the case of PDMS is negative and large, although the enthalpic part of the interaction parameter itself appears to be positive as expected. For the chain lengths examined in our work, Beaucage suggests an isotopic $\chi \sim -5 \times 10^{-3}$. Since the solubility parameter approach described above only works in the case of positive χ values, it appears that this methodology cannot be successfully applied to the problem of interest.

Therefore, we are forced to conclude that current ideas, which use the solubility parameter approach, cannot be used to rationalize the strong isotope dependence of the pressure dependence of the interaction parameter in this case. It is possible, as suggested by Beaucage *et al.*,[20] that the changes in coil dimensions on blending in the case of these siloxane polymers[21] might play a critical role in this case. We conjecture that such changes in chain dimensions might be important since the two classes of blends which have observed negative volume changes on mixing both involve siloxane based polymers.[2] Apart from these conjectures we offer no conclusive understanding of the results reported in this paper.

To address the second issue, we plot the $\underline{\nu}$ values as a function of $\chi(P=0)$, as suggested by Lefebvre *et al.*[7] It is clear that, while the data from any one system appears to follow a linear dependence between these quantities, the three different sets of experimental data for the siloxane blends do not superpose [Fig. 7(c)]. To seek a better understanding of this situation, we have replotted Fig. 7(c), but now including data from the polyolefin blends from Lefebvre *et al.*,[7] the PEE/PDMS blend data from Schwahn *et al.*[2] and those from this work. Due to the large disparity in chain lengths considered in these different works, i.e., $N \approx 2000$ for the polyolefins, ≈ 30 for the PEE/PDMS, and ≈ 200 for the PDMS/PEMS blends the relevant ranges of χ values examined, and hence the thermodynamic states referred to, are quite different.

To normalize these differences, Fig. 8 uses an x-axis of χN. Several important points are highlighted by this figure. First, note that the three different blends have very different values for the $\underline{\nu}$, and its dependence on $\chi(P=0)$. This immediately suggests that the role of pressure on system thermodynamics is much more rich than previously thought. Rather, this figure argues persuasively against the applicability of any universal, one parameter corresponding states principle for describing the role of pressure on blend thermodynamics. Second, note that, at any given $\chi(P=0)$ value, the $|\underline{\nu}|$ value decreases with increasing chain length. Thus, as may be expected from an equation of state model,[5,22] data on volume changes must be considered in the context of their degree of polymerization. Considering plots of $\underline{\nu}$ vs $\chi(P=0)$, as in Ref. 7, which ignore the role of this important variable in both axes, will not collapse experimental data in a universal manner. Third, it is clear that the $\underline{\nu}$ value from the PEE/PDMS blend (obtained from SANS) is 2–3 larger in magnitude than the corresponding data from the PEMS/PDMS blend (using light scattering). The fact that SANS and light scattering on different systems yield qualitatively similar results gives us considerable faith that we are not picking up artefacts in either one probe. Finally, data from the three PEMS/PDMS blends collapse better onto a straight line when examined as a function of χN, than as a function of χ. This argues one more time that $\chi(P=0)$ cannot be the most appropriate variable if one attempts to obtain universal plots describing the relationship between volume changes on mixing and system energetics.

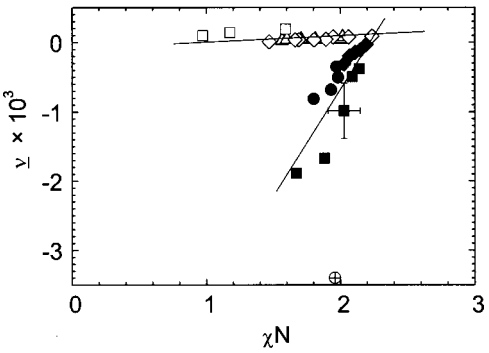

FIG. 8. Plots of $\underline{\nu}$ vs $\chi(P=0)N$ for the siloxane blends (solid points) in this work, the polyolefin blends (open symbols) from Lefebvre *et al.* (Ref. 7) and the PEE/PDMS blend ($\oplus$) from Schwahn *et al.* (Ref. 2). The lines are guides to the eye.

V. CONCLUSIONS

We have measured the pressure dependence of the interaction parameter for various combinations of isotopically labeled PEMS/PDMS blends. Our data, in combination with other sets of experimental data in the literature on blends of polyolefins, and a mixed polyolefin/siloxane blend persuasively argue that the role of pressure on system thermodynamics is significantly richer than previously anticipated. We clearly observe that, even though the $\underline{\nu}$ values from the polyolefin blends and the siloxane blends vary linearly with $\chi(P=0)$, these dependencies are strongly effected by the chemical nature of the two polymers, and their chain lengths. Since there appear to be no straightforward organizing principles that explain these data, we strongly appeal to theorists to consider this important problem and provide new methodologies for their understanding.

ACKNOWLEDGMENTS

The financial support by EC (940603) is gratefully acknowledged. One of the authors (G.M.) thanks FORTH for

support and hospitality. At Penn State University this research was funded by the National Science Foundation (CTS-9975625) and the Division of International programs (INT-9800092).

[1] M. Beiner, G. Fytas, G. Meier, and S. Kumar, Phys. Rev. Lett. **81**, 594 (1998).
[2] D. Schwahn, H. Frielinghaus, K. Mortensen, and K. Almdal, Macromolecules **34**, 1694 (2001).
[3] W. Theobald and G. Meier, Phys. Rev. E **51**, 5776 (1995).
[4] D. Schwahn, T. Schmackers, and K. Mortensen, Phys. Rev. E **52**, R1288 (1995); S. Janseen, D. Schwahn, K. Mortensen, and T. Springer, Macromolecules **26**, 5587 (1995); B. Hammouda, N. P. Balsara, and A. A. Lefebvre, *ibid.* **30**, 5572 (1997).
[5] J. Dudowicz and K. Freed, Macromolecules **28**, 6625 (1995); D. J. Walsh and S. Rostami, *ibid.* **18**, 216 (1985); B. Rudolf and H. J. Cantow, *ibid.* **28**, 6595 (1995).
[6] Compatibilization in polymer–solvent systems by applying pressure has been reported otherwise and was especially emphasized by B. A. Wolff and J. Blaum, J. Polym. Sci., Part C: Polym. Symp. **61**, 251 (1977).
[7] A. A. Lefebvre *et al.*, Macromolecules **32**, 5460 (1999).
[8] P. J. Flory, *Principles of Polymer Chemistry* (Cornell University Press, Ithaca, 1953); P. G. de Gennes, *Scaling Concepts in Polymer Science* (Cornell University Press, Ithaca, 1979).
[9] S. K. Kumar, Macromolecules **33**, 5285 (2000).
[10] G. Scatchard, Trans. Faraday Soc. **30**, 160 (1937).
[11] J. H. Hildebrand, *The Solubility of Non-Electrolytes* (Dover, New York, 1964).
[12] M. Rabeony *et al.*, Macromolecules **31**, 6511 (1998).
[13] U. Maschke, T. Wagner, and X. Coqueret, Macromol. Chem. Phys. **193**, 2453 (1992).
[14] G. Fytas, G. Meier, and Th. Dorfmueller, Macromolecules **18**, 993 (1985).
[15] G. Meier, B. Momper, and E. W. Fischer, J. Chem. Phys. **97**, 5884 (1992).
[16] H. Frielinghaus, B. Abbas, D. Schwahn, and L. Willner, Europhys. Lett. **44**, 606 (1998).
[17] H. Benoit, C R. Acad. Sci., Ser. IIb: Mec., Phys. Chim., Astron. **327**, 139 (1999).
[18] H. Götz and B. Ewen (unpublished).
[19] R. Krishnamoorti, Ph.D. thesis, Princeton University, 1994.
[20] G. Beaucage, S. Sukumaran, S. J. Clarson, M. S. Kent, and D. W. Schaefer, Macromolecules **29**, 8349 (1996).
[21] W. Theobald, A. Sans-Pennincks, G. Meier, and T. A. Vilgis, Phys. Rev. E **55**, 5723 (1997).
[22] R. H. Lacombe and I. C. Sanchez, J. Cryst. Growth **80**, 2568 (1978).